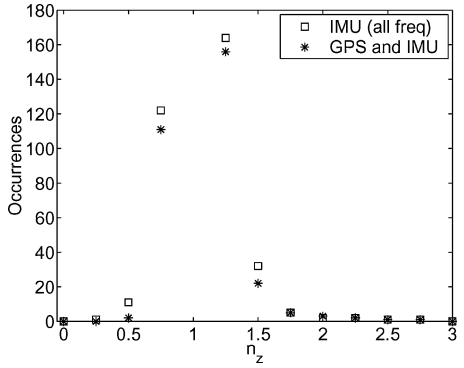

Fig. 2 Load factor occurrences including superimposed IMU data.

To make an estimate of the load factors occurring from gusts, the filtered and randomly chosen $\hat{n}_z^{\mathrm{IMU}}$ from the four altitude segments are superimposed on the calculated n_z^{GPS} before the load factor occurrence program is used. Figure 2 shows the number of load factor occurrences calculated when the $\hat{n}_z^{\mathrm{IMU}}$ is superimposed on n_z^{GPS}. Note that the number of occurrences increases especially for the load factors $n_z = 1.25\ g$ and $n_z = 0.75\ g$, which is due to the superimposed $\hat{n}_z^{\mathrm{IMU}}$ on the GPS maneuver load factor. To resolve the load factor occurrences accurately, the frequency of the IMU data needs to be higher than 15 Hz, preferably even higher than 60 Hz. Nevertheless, a conclusion to be drawn based on Fig. 2 is that the number of occurrences for the GPS data with superimposed reference IMU data agrees rather well with the number of occurrences obtained from just the IMU data.

Summary

To keep the aircraft instrumentation cost down, a method for estimating the load factor history of the SK60 using a GPS receiver and IMU normal acceleration data from a reference aircraft is proposed to keep track of the aircraft usage.

The method of superimposing filtered IMU data from a reference aircraft shows promising results even though the number of flight hours available for this study is limited. The number of occurrences using GPS data with superimposed higher frequency IMU data agrees rather well with the number of occurrences obtained using only the IMU data. It can also be concluded that if the SK60:072 is used in daily training, a larger set of data can be recorded from the IMU. The IMU data can possibly be used to model higher frequency accelerations caused by gusts more accurately by dividing the different flights into not only altitude segments but also into, for example, different weather and aircraft velocity conditions.

The maneuver load factors in this study are assumed to be resolved using 2-Hz GPS data. This can be further improved if a GPS receiver with higher data output rate is used.

Furthermore, the DFT filtering calculations of the higher frequency IMU data are computationally expensive, but in turn, it only needs to be performed once. The calculations using the GPS data assembled with the equations of motion to obtain the load factors and the corresponding occurrences are performed in a few seconds for 1 h of flight.

Acknowledgments

This project is financially supported by the Swedish Defence Materiel Administration. (FMV). The author is supported by Project 246363-LB608644 monitored by Pontus Björk. The opportunity of using the aircraft sensor data has been of great help and thanks are due to Måns Bergmark, Jenni Nylander, Marja-Liisa Nyqvist, and Carlos Bragado Nilsson at FMV.

References

[1]Arrieta, A., and Stritz, A., "Modeling of the Aircraft Fatigue Load Environment," AIAA Paper 2000-0973, Jan. 2000.

[2]Perry, B., III, Pototzky, A. S., and Woods, J. A., "An Investigation of the 'Overlap' Between the Statistical-Discrete-Gust and the Power-Spectral-Density Analysis Methods," NASA TR 89-1376-CP, April 1989.

[3]Farrell, J. A., and Barth, M., *The Global Positioning System and Inertial Navigation*, McGraw–Hill, New York, 1998, pp. 160–164.

[4]de Try, F., "Flight Path Reconstruction Using Numerical Optimization," Dept. of Aeronautics, Technical Rept. 2000-31, Royal Inst. of Technology, Stockholm, May 2000.

[5]De Boor, C., "Package for Calculating with B-Splines," *SIAM Journal on Numerical Analysis*, Vol. 14, No. 3, 1977, pp. 441–472.

[6]Ringertz, U. T., "Multistage Trajectory Optimization Using Large-Scale Nonlinear Programming," Dept. of Aeronautics, Technical Rept. 99-25, Royal Inst. of Technology, Stockholm, Sept. 1999.

[7]Ringertz, U. T., "An Optimal Trajectory for a Minimum Fuel Turn," *Journal of Aircraft*, Vol. 37, No. 5, 2000, pp. 932–934.

[8]Bisplinghoff, R. L., Ashley, H., and Halfman, R. L., *Aeroelasticity*, Addison–Wesley, Cambridge, England, UK, 1955, Chap. 10-7.

[9]Hoblit, F. M., *Gust Loads on Aircraft: Concepts and Applications*, AIAA Education Series, AIAA, Washington DC, 1988, Chap. 11.

Comparisons of a Gurney and Jet Flap for Hingeless Control

Lance W. Traub,* Adam C. Miller,† and Othon Rediniotis‡
Texas A&M University, College Station, Texas 77843-3141

Introduction

ADVANCES in fluidic control have recently raised the proposition of hingeless flow control. For purposes of stealth, reduced vehicle weight, increased robustness, and damage tolerance as well as compactness, the hingeless methodology is extremely attractive. Implementation methods are driven by available fluidic control technology exemplified of late by the synthetic jet actuator (SJA).[1–3] Flow control or manipulation may be achieved through active or passive means; for moment and force augmentation active methods are more feasible. Continuous or oscillatory blowing may be used to suppress separation,[3] "virtually alter the surface,"[4] or cause supercirculation through circulation control effected via trailing-edge and Coanda surface blowing.[5–7] Although it has been demonstrated that control of flow separation can be used for pitch control at high angles of attack,[2] this mechanism is not available or viable at low angles of attack, where aerodynamic efficiency would be marred by large-scale flow separation. At low incidence, the most receptive and effective location for modification to generate pitching moment is the trailing edge. Obvious modifications are the flap. Moments are generated through flap deflection by movement of the rear stagnation point yielding increased vertical momentum transfer. Other trailing-edge modifications are pneumatic; either a jet flap, where a high-velocity jet is issued from the trailing edge at an inclination angle, or a blown flap, where the jet is directed over the flap. All these methods are effective but may require significant quantities of air for operation.

The Gurney flap[8,9] has been shown to be a highly effective small-scale (typically 0.5–1.5% of the chord) modification that can achieve significant lift and pitching moment generation. The flap functions by essentially increasing the downward deflection of the trailing-edge flow, facilitated through the formation of a series of counter-rotating vortices similar to that of a von Kármán vortex street. A

Received 24 October 2003; revision received 18 December 2003; accepted for publication 18 December 2003.

*Texas Engineering Experiment Station Research Scientist, Aerospace Engineering Department.

†Graduate Student, Aerospace Engineering Department. Student Member AIAA.

‡Assistant Professor, Aerospace Engineering Department. Member AIAA.

subsequent effect is an apparent violation of the trailing-edge Kutta condition; experimental data shows that finite loading is carried to the trailing edge. For hingeless flow control the basic tenet (i.e., its small size) of the Gurney flap is attractive, but its implementation would require moving parts. Consequently, this study investigates the moment and lift augmentation capability of a jet flap (operated at comparatively low jet momentum coefficients, C_μ) compared to a typically sized Gurney flap. The data will provide insight into the feasibility of this proven technology to facilitate hingeless control. These tests also serve as a precursor to implementation of an SJA that may provide greater effectiveness coupled with lower required C_μ. This implementation is the subject of ongoing research.

Experimental Details

For initial proof of concept testing, a continuous air supply was implemented using an external high-pressure source. A wing was manufactured from foam and balsa to accommodate the jet. The wing was then covered with heat shrink to ensure a smooth surface. A NACA 0015 profile was used. The wing was equipped with end plates to mimic two-dimensional flow. The width of the slot was 1 mm, giving a slot exit area of 0.0002 m^2. The slot was located 15 mm from the wing's trailing edge. As implemented, the flap is a jet flap, with a large jet inclination (90-deg) angle.

Geometric details of the model are a chord of 0.71 m and a span of 0.235 m. The tests were undertaken in Texas A&M University's 3 by 4-ft closed-loop wind tunnel. A freestream velocity of 15 m/s was used, yielding a Reynolds number of 0.7×10^6. Tunnel turbulence intensity has been measured at less than 0.5% assuming isotropic turbulence. Data acquisition was facilitated using a three-component pyramidal balance. Balance output voltages were read using a 16-bit A/D board. A dedicated software acquisition code has been written for this facility and was used for acquisition and processing. Prior to use for these experiments, the pyramidal balance was recalibrated. Subsequent balance verification through application of pure and combined loads suggests accuracies better then 0.6% for lift, drag, and pitching moment. Wind-tunnel corrections for solid and wake blockage were applied using the methodology described in Ref. 10.

To achieve blowing, shop air was used as the pneumatic source. Slot exit jet momentum coefficients were measured using a British Standard (part 1042) orifice plate. The orifice facilitated the measurement of the mass flow rate, which in conjunction with continuity allowed determination of the jet slot exit velocity. The measurement technique was verified using a TSI calibrator that allows accurate measurement of an air jet exhausting from its settling chamber. Air to the calibrator was supplied through the orifice plate. Slot exit velocities were measured and compared with predictions using the orifice. Agreement was generally within 1.5%.

Results

Force Balance

In all data, the effects of the jet reaction on lift and pitching moment coefficient (C_μ) have been removed through tare runs; consequently, pure aerodynamic loading is shown. Results are summarized in Figs. 1–3. The effects of C_μ (jet velocity × mass flow rate/dynamic pressure × reference area) on the measured lift coefficient (C_l) is shown in Fig. 1. Also included is a plot showing the lift augmentation ratio (upper element). This ratio is defined as $(C_{lC_{\mu\neq 0}} - C_{lC_{\mu=0}})/C_\mu$ for the present jet configuration. The ratio clearly shows how the effectiveness of the jet relates to the supplied momentum. A coefficient greater than 1 indicates that augmentation is greater than if the jet had been used purely for its reactive lift. Also included in the data are results for a 0.75% chord Gurney flap (made from brass shim), which was positioned at the same location as the jet. This is a typical size for a Gurney flap and provides a reference for the lift and moment alteration provided through blowing. The data in Fig. 1 show that the jet flap shifts the angle of attack negatively for zero lift, as does a conventional flap. A momentum coefficient of 0.0068 is seen to provide similar lift augmentation to the gurney flap. The magnitudes of the recorded lift also suggest

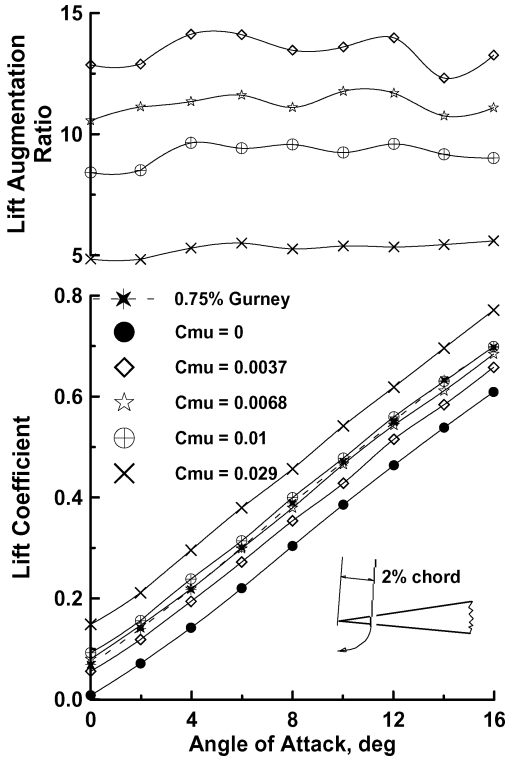

Fig. 1 Effect of C_μ on lift coefficient and lift augmentation ratio.

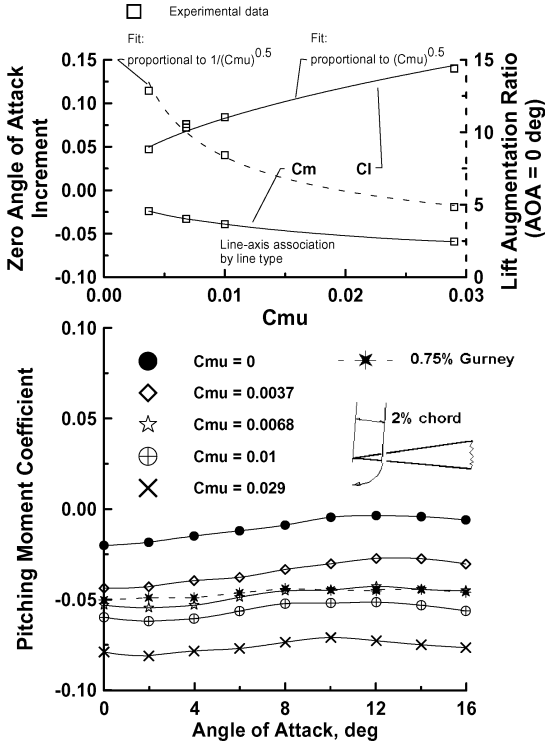

Fig. 2 Effect of C_μ on pitching moment coefficient and zero angle-of-attack increments; moments taken about the quarter chord.

that the endplates were not large enough to ensure two-dimensional flow. Supporting this is the lift curve behavior; there is a nonlinear increase around 4 deg, as seen on low-aspect-ratio plates. However, this does not affect the comparative nature of the data presentation. The effectiveness of the blowing may be gauged by examining the lift augmentation ratio shown in the top of the multipart figure. The jet greatly augments the lift compared to the momentum added to the flow. The greatest augmentation is seen for lower C_μ; increasing

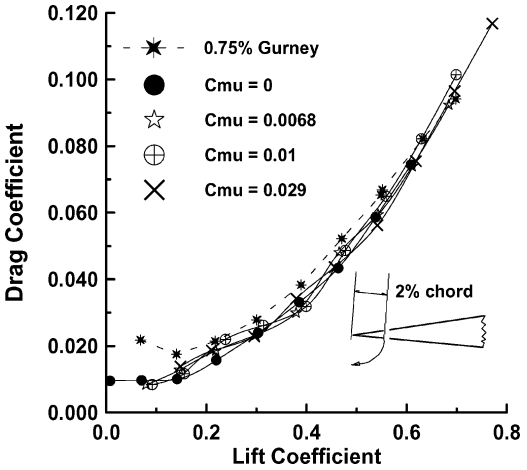

Fig. 3 Effect of C_μ on drag coefficient.

the jet's momentum reduces the relative benefit if not the magnitude of the augmentation. The augmentation ratios are of similar magnitude to those calculated by Lockwood and Vogler.[11]

In the present application, the primary focus of the effect of the jet is in its impact on moment, so as suitable for hingeless control. The negative shift of the pitching moment curve (moments taken about the quarter chord), typical of a trailing-edge flap, is clearly seen in Fig. 2. As noted for lift, the zero-lift pitching moment caused by $C_\mu = 0.0068$ is comparable to that generated by a 0.75% chord Gurney flap. The magnitudes of the moment generated, although toward the low end of what a conventional trailing-edge flap may generate, are sufficient for pitch control at low angles of attack. However, the required jet momentum coefficients may be slightly excessive for actual implementation.[12] Pitch control could be achieved by locating a jet slot on the upper and lower surface, which allows control of the vehicles' incidence. Also shown in Fig. 2 are the dependencies of the zero lift increments of C_μ and C_l as well as the lift augmentation ratio on the jet momentum coefficient. As may be seen, the greatest augmentation occurs at the lowest C_μ, with the increment appearing to monotonically approach a bound for increasing C_μ. Analytic expressions due to Spence[13] suggest a dependency proportional to $C_\mu^{0.5}$ for C_l and $1/C_\mu^{0.5}$ for the lift augmentation ratio. Curve fits of the experimental data using these functional dependencies are also included in the figure. Although Spence's theory is for low C_μ and small jet deflection angles, the data clearly show that Spence's theoretical relations are still valid (in trend if not exact magnitude) for extreme jet angles.

Effects of the trailing-edge devices on the measured drag coefficient are presented in Fig. 3. The data show that the Gurney flap incurs a zero-lift drag penalty, which diminishes at higher lift coefficients, a result noted by other researchers.[9] The jet flaps have no experimentally significant effect on the recorded drag coefficient. These data suggest that although the Gurney and jet flap ($C_\mu = 0.0068$) have similar performance, the jet flap is not hindered by a drag penalty at low incidence. It does, however, have the expense of requiring high-pressure air. Calculations of power required indicate that at low incidence the jet flap configuration ($C_\mu = 0.0068$) requires 10% less total power (drag plus jet) than the Gurney flap (drag). However, as incidence increases this advantage is lost (e.g., at $C_l = 0.55$, the jet flap requires 5.5% more power).

Flow Visualization

To gain an insight into the similarities/differences of the trailing-edge flow physics between the Gurney and jet flap, flow visualization using titanium dioxide was used. A thin plate was attached parallel to the side plates. Visualization of the skin friction lines on the streamwise plate would then give an approximate indication of the streamline patterns. Note that, due to the effects of gravity on the fluid medium as well as the viscosity of the Kerosene, the data are purely qualitative and no inferences should be made as to precise locations or trajectories of flow features. Figure 4 presents acquired images for the 0.75% Gurney flap and jet flap ($C_\mu = 0.01$) at a freestream velocity of 15 m/s. From the data we infer that, despite similar aerodynamic effect, the flow physics present are somewhat dissimilar. The jet flap shows evidence of significant turning of the flow around the trailing edge such that the jet exit becomes functionally the rear separation line. The jet is seen to expand rapidly and deflect streamwise, initially due to pressure gradients across the jet and later due to entrainment and absorption of the freestream axial momentum.[14] Notice the half-saddle aft of the trailing edge demarcating the dividing streamline between fluid drawn around the trailing edge and that drawn down and streamwise. The Gurney flap appears to shed a fairly thick wake extending from the separation bubble formed behind the flap. The visualized wake may correspond to the von Kármán vortex street identified by Jeffrey et al.[8] The significant turning of the flow seen with the jet flap is not observed. A line indicating the approximate trajectory of the shear layer shed from the flap extremity is also observed. Comparison of the skin friction patterns also suggests that, whereas the jet flap draws the lower surface boundary layer away from the surface,[14] the Gurney causes deceleration and recompression. It may thus be tentatively inferred that the Gurney augments lift by violating the Kutta condition whereas the jet flap increases flow turning and, hence, effective camber near the trailing edge.

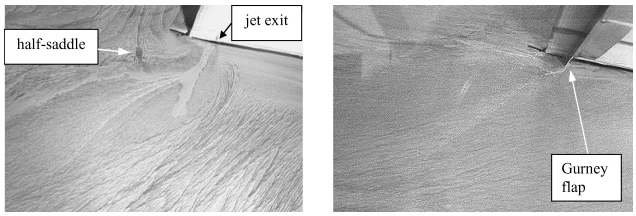

Fig. 4 Streamwise flow patterns.

Conclusions

A preliminary wind-tunnel investigation was undertaken to examine the possibility of using a jet flap for hingeless control. Tests encompassed jet momentum coefficient variation and comparison with a Gurney flap located at the same location. The data showed that the jet flap generates lift and moment coefficient increments similar to a 0.75% chord Gurney flap for moderate jet momentum coefficients. However, whereas the Gurney flap showed a zero-lift drag coefficient penalty, this was not present for the jet flap. Analysis showed that the power required by the jet flap airfoil for similar lift and moment increments was less than that required for the Gurney flap airfoil at low incidence—this trait reverses at higher incidence.

References

[1]Gilarranz , J. L., Traub, L. W., and Rediniotis, O. K., "Characterization of a Compact, High-Power Synthetic Jet Actuator for Flow Separation Control," AIAA Paper 2002-0127, Jan. 2002.

[2]Traub, L. W., Miller, A., and Rediniotis, O., "Effects of Synthetic Jet Actuation on a Pitching NACA 0015," *Journal of Aircraft* (accepted for publication).

[3]Amitay, M., and Glezer, A., "Role of Actuation Frequency in Controlled Flow Reattachment over a Stalled Airfoil," *AIAA Journal*, Vol. 40, No. 2, 2002, pp. 209–216.

[4]Smith, D., Amitay, M., Kibens, V., Parekh, D., and Glezer, A., "Modifications of Lifting Body Aerodynamics Using Synthetic Jet Actuators," AIAA Paper 98-0209, Jan. 1998.

[5]Englar, R. J., "Circulation Control for High Lift and Drag Generation on STOL Airfoil," *Journal of Aircraft*, Vol. 12, No. 6, 1975, pp. 457–463.

[6]Englar, R. J., Trobaugh, L. A., and Hemmerly, R. A., "STOL Potential of the Circulation Control Wing for High Performance Airfoil," *Journal of Aircraft*, Vol. 15, No. 3, 1978.

[7]Kind, R. J., and Maull, D. J., "An Experiment Investigation of a Low-Speed Circulation Controlled Aerofoil," *Aeronautical Quarterly*, Vol. 19, May 1968, pp. 170–182.

[8]Jeffrey, D., Zhang, X., and Hurst, D. W., "Aerodynamics of Gurney Flaps on a Single-Element High-Lift Wing," *Journal of Aircraft*, Vol. 37, No. 2, 2000, pp. 295–301.

[9]Papadakis, M., Myose, R. Y., Heron, I., and Johnson, B. L., "An Experimental Investigation of Gurney Flaps on a GA(W)-2 Airfoil with 25% Slotted Flap," AIAA Paper 96-2437, 1996.

[10]Rae, W., and Pope, A., *Low-Speed Wind Tunnel Testing*, Wiley, New York, 1984, pp. 344–401.

[11]Lockwood, V. E., and Vogler, R. D., "Exploratory Wind-Tunnel Investigation at High Subsonic and Transonic Speeds of Jet Flaps on Unswept Rectangular Wings," NACA TN 4353, Aug. 1958.

[12]Wood, N. J., Sadri, A. M., and Crook, A., "Control of Turbulent Flow Separation by Synthetic Jets," AIAA Paper 2000-4331, Aug. 2000.

[13]Spence, D. A., "Some Simple Results for Two-Dimensional Jet-Flap Aerofoils," *Aeronautical Quartely*, Nov. 1958, pp. 395–406.

[14]Jordinson, R., "Flow in a Jet Directed Normal to the Wind," Research & Memoranda (R&M) 3071, London, Oct. 1956.